Sensors & Transducers, Vol. 270, Issue 3, November 2025, pp. 79-87

www.sensorsportal.com

Sensors & Transducers

Published by IFSA Publishing, S. L., 2025
http://www.sensorsportal.com

Enhanced SUMO–VLC Framework for Real-time Vehicular Communication and Validation

[1, 2, *] Paula LOURO, [1] Gonçalo GALVÃO, [1] Afonso GASPAR, [1] João DRAGOVIC, [1] João MARQUES, [1, 2, 3] Manuela VIEIRA and [1, 2] Manuel Augusto VIEIRA

[1] Electronics Telecommunication and Computer Dept. ISEL,
R. Conselheiro Emídio Navarro, 1959-007 Lisboa, Portugal
[2] UNINOVA –CTS and LASI, Quinta da Torre, Monte da Caparica, 2829-516, Caparica, Portugal
[3] NOVA School of Science and Technology, Quinta da Torre, Monte da Caparica, 2829-516, Caparica, Portugal
Tel.: +351 218317000
E-mail: paula.louro@isel.pt

Received: 2 June 2025 / Revised: 11 Nov. 2025 / Accepted: 19 Nov. 2025 / Published: 28 Nov. 2025

Abstract: This work explores the integration of visible light communication technology with urban traffic management systems. Using RGBV LEDs, Visible Light Communication facilitates real-time data collection – such as vehicle position, speed, queue length, and waiting time – through transmitters embedded in streetlights, traffic signals, and vehicle headlights. These enable multiple communication modes: vehicle-to-vehicle vehicle-to-infrastructure), infrastructure-to-vehicle and lamp-to-vehicle. The system is simulated using the "Simulation of Urban Mobility traffic" simulator, replicating realistic vehicle dynamics and visible light communication-based data exchange. Communication channels operate using On-Off Keying modulation, transmitting 64-bit frames structured according to a defined visible light communication protocol.
A key contribution of this work is the development of signal pre-processing and decoding algorithms at the receiver module. These algorithms demultiplex the composite optical signal received by the photodetector, enabling identification of the emitting sources and reliable data extraction. Signal processing techniques include baseline correction using asymmetric least squares smoothing, correction of capacitive effects, and transient noise filtering based on signal slope analysis. By integrating the traffic simulator outputs with the visible light communication system, the approach aims to enhance traffic monitoring, reduce congestion, and support the future integration of visible light communication into smart transportation infrastructure. This integration demonstrates the potential of combining advanced error correction techniques with traffic simulation data to improve urban communication infrastructures.

Keywords: Visible light communication, Traffic management, Signal decoding, Simulation of urban mobility, Connected vehicles.

1. Introduction

The escalating complexity of urban transportation necessitates the evolution of traffic management systems toward more intelligent and efficient infrastructures [1, 2]. Visible Light Communication (VLC) emerges as a viable solution, enhancing existing LED-based lighting infrastructure to provide high-speed data transmission without interfering with the radio-frequency spectrum [3]. By modulating the intensity of light emitted from LEDs, VLC enables optical communication, making it particularly suitable for urban environments where LEDs are prevalent in road environments with streetlights, traffic signals, and vehicles [4, 5].

This study investigates the application of VLC in urban traffic management by simulating various traffic scenarios using the Simulation of Urban Mobility (SUMO) platform [6]. The simulation replicates realistic vehicle dynamics and assesses VLC-based communication links under diverse traffic conditions. The communication protocol implemented uses On-Off Keying (OOK) modulation to transmit information in 64-bit frames, conveying essential traffic data such as vehicle position, speed, queue length, and waiting time [7].

In addition to enabling high-speed communication, VLC can also support accurate vehicle localization in urban environments [8, 9]. By exploiting the spatially confined propagation of visible light and the known positions of LED sources, such as streetlights, traffic signals, and vehicle headlights, VLC allows the estimation of vehicle positions with high precision. Techniques such as Received Signal Strength (RSS) measurements [10], Angle of Arrival (AoA) [11], and time-based methods can be employed to derive location information, providing a complementary function to traditional GPS systems, particularly in dense urban areas where GPS signals are often degraded [12]. This dual capability of VLC, simultaneous communication and localization, enhances traffic management systems by enabling real-time monitoring of both vehicle state and position, facilitating more precise routing, collision avoidance, and dynamic traffic coordination.

A central challenge VLC of systems is the reliable extraction of transmitted information from noisy, multiplexed optical signals received by photodetectors [13, 14]. To address this, the study focuses on developing advanced signal pre-processing and decoding algorithms. Initially, clustering algorithms are applied to define decision thresholds, facilitating the mapping of analog signal levels to digital bit values [15]. Further signal processing techniques include baseline correction using asymmetric least squares smoothing, compensation for capacitive coupling effects, and noise suppression based on signal slope analysis [16].

As part of the developed work, the VLC prototype was integrated with the traffic simulator (SUMO). Traffic information from a specific urban scenario was extracted from SUMO and directed to the VLC prototype. This data was encoded using a dedicated communication protocol and used to operate the VLC transmitter. The resulting electrical signals, captured by the photodetector, were recorded for subsequent processing and decoding. This integration enhances the assessment of VLC's effectiveness in real-time traffic monitoring and management within simulated urban environments.

Compared to existing works and our previous study [17], which focused on a VLC-based dual-purpose communication and localisation system, this manuscript presents a refined framework with updated references, an enhanced introduction, new results and a newly developed methodology for VLC-enabled urban traffic management.

2. Methodology

This study develops a VLC-enabled traffic management framework for vehicles operating in urban environments. The proposed workflow comprises a sequence of steps designed to model, monitor, and optimise vehicular operations, from route allocation to real-time traffic coordination.

Initially, vehicle routes are assigned according to the urban road network layout, which includes streets and intersections. This allocation process considers both spatial constraints and traffic priorities to ensure realistic and efficient mobility patterns. Once defined, vehicular movements are modelled using the Simulation of Urban Mobility (SUMO) platform. SUMO provides a microscopic simulation of vehicle dynamics, capturing parameters such as position, velocity, acceleration profiles, queue lengths, and lane-changing behaviour. Various simulation scenarios are generated by adjusting vehicle densities, traffic signal cycle durations, and network complexities to examine system performance under diverse traffic conditions.

The simulation outputs are subsequently transmitted and decoded using the VLC-enabled communication system. The VLC link is modelled as a high-speed, low-latency communication channel capable of broadcasting positional and traffic data from vehicles to the central traffic management unit. Through this channel, critical state information – including vehicle positions, lane occupancy, and intersection queue lengths – is delivered in real time, enabling continuous situational awareness across the traffic network.

3. Integrated Urban Simulation and Vehicular Communication with VLC

The proposed intelligent traffic management system takes advantage of VLC to enable real-time monitoring and control of urban mobility. Traffic information such as vehicle position, speed, queue length, and waiting times are first generated by the SUMO simulator.

These data are encoded and transmitted via VLC transmitters integrated into both infrastructure elements (e.g. lamp posts and traffic lights) and vehicles. VLC receivers, embedded in mobile units or roadside devices detect and decode the optical signals to recover the transmitted traffic information.

An intelligent agent processes the recovered traffic data and makes optimal control decisions based on pre-defined algorithms. These decisions can also be used to train a neural network, progressively enhancing the agent's future responses. The complete data acquisition, communication, processing, and control flow is depicted in Fig. 1, illustrating the interaction between the mobility simulation, VLC communication infrastructure, and the intelligent control system.

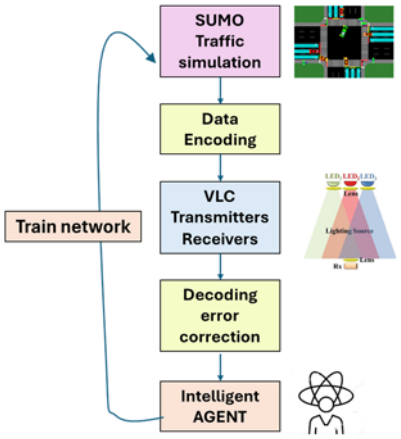

Fig. 1. End-to-end VLC-enabled traffic management pipeline.

3.1. Traffic Simulation with SUMO

The process begins with the simulation of urban mobility using SUMO, enabling the detailed modelling of individual vehicle and pedestrian behaviours within complex road networks.

In this work, the simulated network consists of two homogeneous intersections, each configured with four arms, illustrated in Fig. 2. Each arm includes two dedicated lanes: one lane for through movements and right turns, and a separate lane exclusively for left-turn maneuvers. This layout is specifically designed and optimized for Connected Autonomous Vehicles (CAVs), which, due to their continuous awareness of intended routes, can position themselves in the correct lane in advance, thereby minimizing lane-changing behavior and enhancing traffic efficiency. The scenario also incorporates sidewalks to account for pedestrian movements, ensuring a more comprehensive and realistic representation of urban traffic dynamics.

To emulate the deployment of Visible Light Communication (VLC) infrastructure, lamp posts equipped with VLC transmitters are positioned along the sidewalks at regular intervals of 30 metres. This arrangement defines the VLC coverage zones (or footprints) along each lane, simulating the spatial availability of the communication channel. These VLC footprints serve as the physical layer interface for data exchange between the infrastructure and mobile receivers, enabling the evaluation of signal availability, decoding performance, and communication reliability under realistic mobility conditions.

3.2. Encoding and VLC Transmission

In the simulated urban environment, the movement of vehicles and pedestrians generates dynamic traffic information. This data – such as position, speed, queue length, and waiting time – is extracted from the SUMO simulator and used to emulate VLC communication scenarios along the road network. For each communication event, the traffic data is encoded into digital frames according to a predefined VLC protocol (Table 1).

These frames, comprising 64-bit sequences, are structured to represent different communication contexts and are subsequently modulated using On-Off Keying (OOK). Although higher-speed VLC schemes such as OFDM or CSK were not explored, the use of OOK is entirely appropriate for traffic management applications. The data rate afforded by OOK is sufficient to meet the temporal requirements for encoding and transmitting control information, such as traffic light states and basic signalling. Given that decision cycles in traffic control typically occur on the scale of seconds, the adoption of a simple, robust, and energy-efficient modulation scheme like OOK is both practical and well justified.

Once generated, the VLC frames are transmitted via VLC emitters embedded in infrastructure and vehicles, such as streetlights, traffic signals, and vehicle headlights. This architecture supports multiple communication modes essential to smart mobility systems: Vehicle-to-Vehicle (V2V), Vehicle-to-Infrastructure (V2I), Infrastructure-to-Vehicle (I2V) and Lamp-to-Vehicle (L2V), as illustrated in Fig. 3.

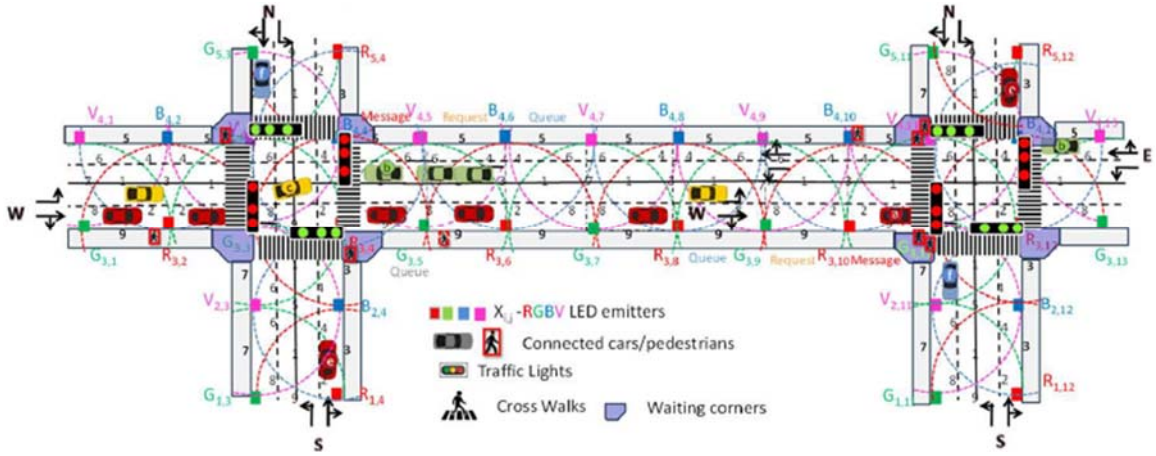

Fig. 2. Traffic environment composed by two four-arm intersections.

Table 1. Message protocol for each of VLC communications.

	SOF	TIME			FLAG	COM	POSITION		PAYLOAD							EOF
	5 bits	6 bits	6 bits	6 bits	4 bits	4 bits	4 bits	4 bits	4 bits	4 bits	4 bits	4bits	4 bits	4bits	... bits	4bits
L2V	Sync	Hour	Min	Sec	END	1	y	x								EOF
V2V	Sync	Hour	Min	Sec	END	2	y	x	Lane (0–7)	Veic. (nr)	Car IDx	Car IDy	nr behind			EOF
V2I	Sync	Hour	Min	Sec	END	3	y	x	TL (0–15)	Veic. (nr).	Car IDx	Car IDy	nr behind			EOF
I2V	Sync	Hour	Min	Sec	END	4	y	x	TL (0–15)	ID Veic.	Car IDx	Car IDy	nr behind	Phase		EOF
P2I	Sync	Hour	Min	Sec	END	5	y	x	TL (0–15)	Direct.	payload					EOF
I2P	Sync	Hour	Min	Sec	END	6	y	x	TL (0–15)	Phase	Payload					EOF

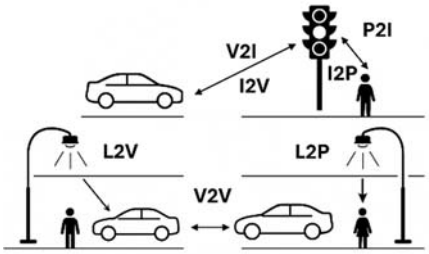

Fig. 3. VLC communication modes.

3.3. Optical Reception, Signal Processing, and Information Recovery

The modulated optical signals transmitted by VLC emitters are received by photodetectors installed on vehicles or within fixed infrastructure.

At the receiver module, the captured signal undergoes a series of signal pre-processing and decoding operations to ensure accurate extraction of the transmitted data. The processing pipeline includes:

- Baseline correction using asymmetric least squares smoothing, which compensates for slow-varying signal drift;
- Correction of capacitive effects, which are typically introduced by the electronic components of the acquisition system;

Transient noise filtering based on slope analysis, designed to suppress high-frequency disturbances and isolate valid signal transitions.

Fig. 4 illustrates the different stages from optical reception to error correction and data recovery in the VLC-based traffic system.

Once the signal has been adequately conditioned, a parity-based error control mechanism is applied. This strategy enables the detection and correction of transmission errors, thereby increasing the robustness and reliability of the communication channel. Finally, the decoded data is used to reconstruct the original traffic parameters generated by the SUMO simulator.

3.4. Experimental VLC setup and Data Collection

To validate the proposed VLC-based V2X communication protocol, a simulation–experiment integration was developed. The SUMO traffic simulator was fully integrated with the VLC-based communication system, enabling vehicles to interact in real time with the proposed framework. The simulation provided continuous updates of vehicle positions, velocities, and intended manoeuvres, which were transmitted through the different communication channels.

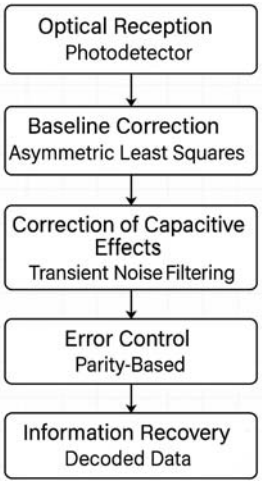

Fig. 4. VLC Signal processing pipeline.

The communication protocol employed four VLC channels: L2V for vehicle localisation, V2V for exchanging information on movement, position, and operational state, V2I for requesting intersection crossings, and I2V for transmitting traffic signal phase information. This configuration enabled the collection of channel-specific performance data under realistic urban traffic conditions, including stopping times, intersection waiting times, and overall traffic throughput.

Through this integration, the SUMO-based framework reproduced the dynamics of a representative urban traffic network while allowing for quantitative validation of the VLC-based V2X protocol. The results demonstrated that coordinated V2V and V2I communication, complemented by adaptive I2V control, significantly reduced traffic congestion and improved vehicular flow efficiency across the simulated network.

4. Results and Discussion

4.1. Simulation Scenario

A 32-second simulation was configured in SUMO, featuring two vehicles approaching and passing through an intersection. This scenario allows the observation of four distinct frame types; however, in this article, we focus only on the L2V and V2V communication channels. At the 2-second mark, Fig. 5 illustrates the first communication event, triggered when a vehicle (represented in red) enters the coverage area of a streetlight (depicted by green walls), thereby initiating L2V communication.

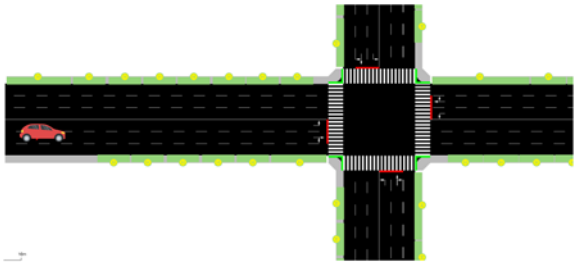

Fig. 5. Second 2 of the simulation.

The electrical signal generated by the photodiode in response to the optical excitation carrying the frame is observed on the oscilloscope, as shown in Fig. 6.

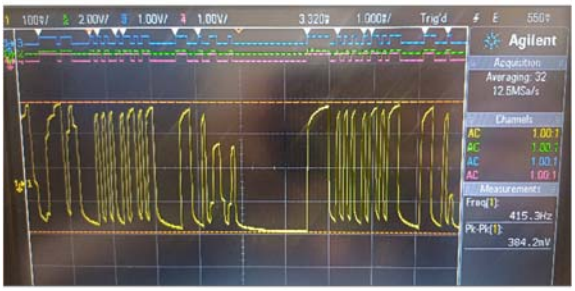

Fig. 6. L2V frame displayed on the digital oscilloscope.

In the yellow signal observed on the oscilloscope shown in Fig. 6, the synchronisation block can be identified, followed by the information blocks of the L2V communication: timestamp, flag, position, and payload (empty as indicated in the coding protocol of Table 1). Above it, the signals transmitted by the LEDs encoding the frame are also visible.

The introduction of the second vehicle at the 31-second mark enables the V2V communication, expanding the scope of the simulation beyond the initial L2V interactions. This event is triggered when the second vehicle approaches within 40 metres of the first, as illustrated in the traffic scenario modelled in SUMO (Fig. 7), where the second vehicle is depicted in blue.

The additional data captured in Fig. 8 demonstrate the transmission of V2V frames, as electrical signals on the oscilloscope.

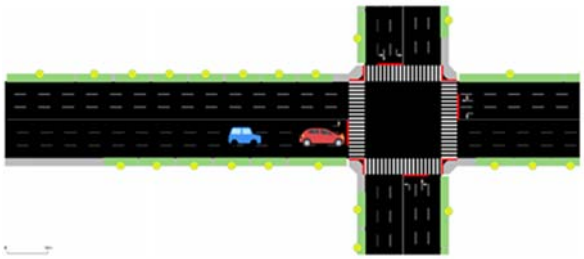

Fig. 7. Second 31 of the simulation.

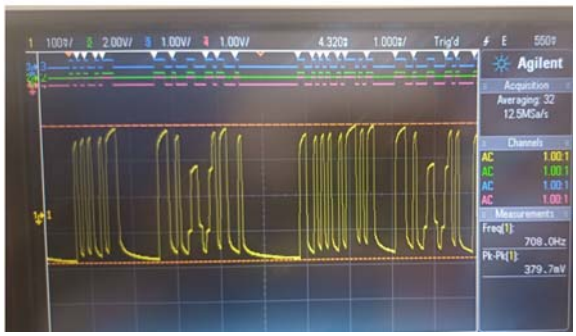

Fig. 8. V2V frame displayed on the digital oscilloscope.

The V2V communication frames include critical information exchanges that facilitate vehicle-to-vehicle awareness, which is essential for cooperative driving and collision avoidance systems.

Besides the synchronization block, the message includes a timestamp, a flag, position information, and a payload containing specific data related to the current lane – such as the number of vehicles behind the leading vehicle and the corresponding identification of those vehicles. This identification is obtained through L2V and gathered via the V2V communication chain, allowing for an accurate estimation of both queue length and vehicle distribution within the lane. This enables the estimation of queue length and waiting times. The leading vehicle – defined as the first vehicle in the queue closest to the traffic light – transmits this information via V2I communication to the intelligent traffic agent.

Each intersection is composed of four arms, as illustrated in Fig. 2. The traffic agent receives information from each of these arms, including the positions of vehicles on the lanes, thereby obtaining an accurate estimation of the queue lengths. Based on this data, the agent activates the most appropriate signal phase to optimize vehicle flow through the intersection. Moreover, the collected traffic data can be used to train the agent to make increasingly better decisions, by learning from the observed traffic

patterns in real time – making the system progressively more adaptive to current traffic conditions. Given the high volume of detailed traffic data that can be gathered, the agent can also be trained to follow specific traffic management strategies when necessary, such as prioritizing East–West or North–South movements, depending on predefined objectives or dynamic traffic demands.

The electrical signal captured by the photodiode, as shown on the oscilloscope screens in Figs. 6 and 8, requires decoding to retrieve the transmitted information. The following section outlines the signal processing steps used, highlighting the most critical stages.

4.2. Signal Recovery

To reduce residual light interference at the receiver, baseline correction was performed using the Asymmetric Least Squares (AsLS) method. This iterative algorithm fits a smooth baseline by penalising positive and negative deviations asymmetrically, effectively separating the signal from background noise. Fig. 9 shows the photocurrent signal acquired from a V2V link before and after baseline correction using the AsLS method.

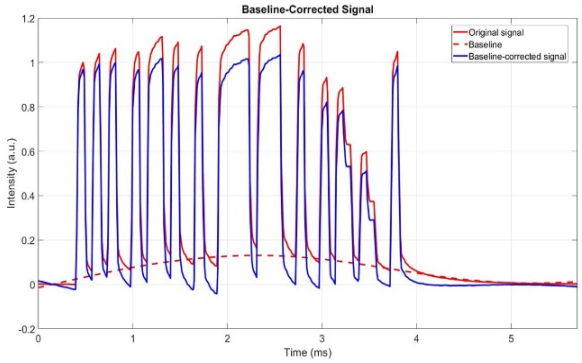

Fig. 9. Original (black) vs. baseline-corrected signal (blue) using AsLS.

The raw signal (black) contains drift and noise components that obscure the digital transitions. After processing (blue), the baseline is removed, enhancing the visibility of signal transitions and enabling accurate thresholding for bit decoding. This improvement was essential for recovering the original frame with minimal error.

The signal from the photodiode shows a capacitive effect due to the p-n junction's inherent capacitance, which limits its response speed. Applying reverse bias reduces this capacitance by widening the depletion region, improving response time, but cannot eliminate it entirely. Consequently, the signal transitions between light and dark states are gradual, producing rounded edges instead of sharp changes.

To address this, a segmented correction method was applied. It detects and adjusts overshoot and undershoot deviations within each time interval, applying accumulated corrections and storing any excess or deficit for correction in the next interval. This iterative correction progressively minimises discrepancies from abrupt signal changes, enhancing data uniformity and fidelity. The corrected signal is then mapped to its corresponding levels, as shown in Fig. 10.

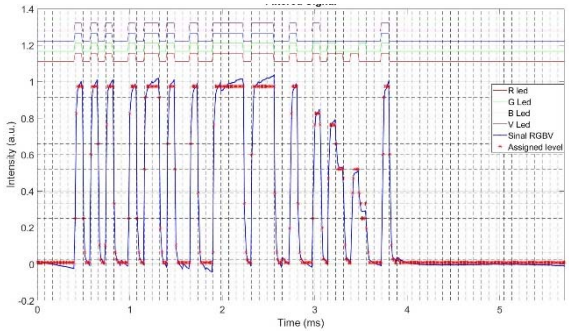

Fig. 10. Filtered signal after capacitive effect compensation.

The performance of these techniques was evaluated using signals from various communication links. Fig. 11-13 present the raw signals measured in the L2V, V2V and V2I links, alongside the corresponding processed signals.

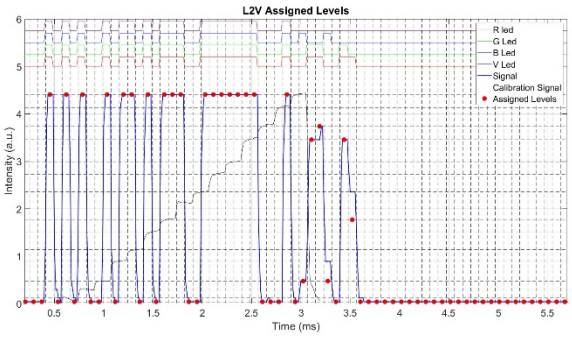

Fig. 11. Photocurrent signal obtained in a L2V link.

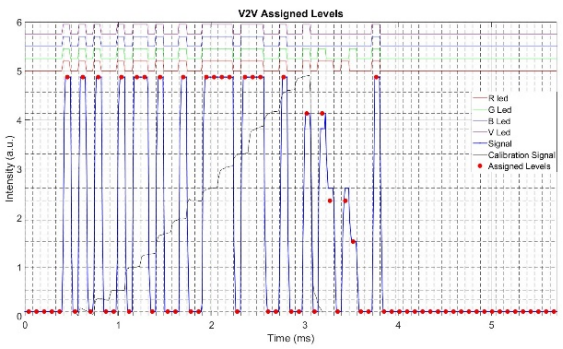

Fig. 12. Photocurrent signal obtained in a V2V link.

The process of decoding the transmitted frame relies on a calibration signal comprising 16 distinct photocurrent levels at the photodetector, achieved by appropriately adjusting the LED driving currents. Fig. 14 presents this calibration signal, with each level corresponding to a specific input optical state. The optical signals emitted by each LED are shown at the top of the figure.

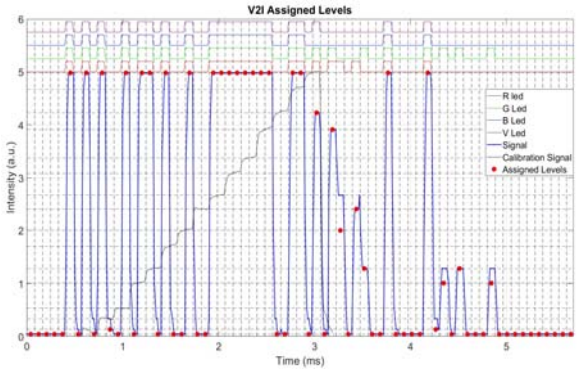

Fig. 13. Photocurrent signal obtained in a V2I link.

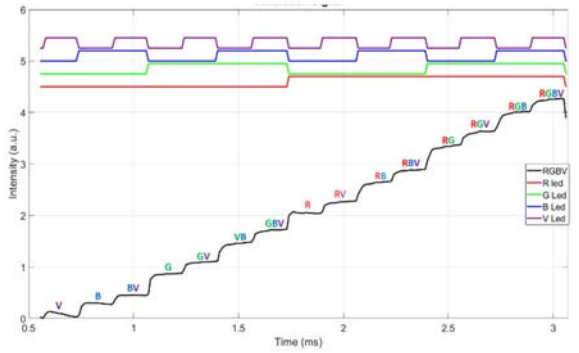

Fig. 14. Experimental calibration signal and representation of the modulated signal of each LED.

The calibration method relies on generating 16 distinct photocurrent levels at the photodetector, each corresponding to a unique combination of the four optical emitters. These levels form a reference signal (as shown in Fig. 14) used in the first decoding stage, where received signals are mapped to the nearest calibrated level.

However, when photocurrent levels are too close, due to noise or non-linearities, decoding errors may occur, increasing the bit error rate. To improve reliability, signal preprocessing is applied before decoding, including baseline correction, noise filtering, and compensation for distortions. These steps help align the received signal with the calibration reference, enhancing decoding accuracy.

In Table 2, the frame transmitted in the L2V link is shown alongside the corresponding decoded signal obtained through the preprocessing techniques.

The error occurred during the decoding of the L2V frame, resulted four incorrect bit assignments. This discrepancy is shown in Table 2, with correct bits highlighted in green and decoding errors marked in red.

Table 3 presents the frame transmitted over the V2V link, together with the corresponding decoded signal obtained via the applied preprocessing techniques.

Table 2. Transmitted and decoded data of the L2V link.

Transmitted Frame
0C21 0000 0C21 0000 0C21 0000 0000 0C21 0000 0C21 0C21 0000 0C21 0000 0C21 0C21 0C21 0000 0000 0C21 0C21 0C21 0C21 0C21 0C21 0C21 0000 0000 0000 0C21 0000 0400 0021 0021 0400 0000 0021 0001 0000 0000 0000 0000 0000 0000 0000 0000 0000 0000 0000 0000 0000 0000 0000 0000 0000 0000 0000 0000 0000 0000 0000 0000 0000 0000
Decoded Frame
0C21 0000 0C21 0000 0C21 0000 0000 0C21 0000 0C21 0C21 0000 0C21 0000 0C21 0C21 0C21 0000 0000 0C21 0C21 0C21 0C21 0C21 0C21 0C21 0000 0000 0000 0C21 0000 0C00 0021 0821 0C00 0000 0021 0C20 0000 0000 0000 0000 0000 0000 0000 0000 0000 0000 0000 0000 0000 0000 0000 0000 0000 0000 0000 0000 0000 0000 0000 0000 0000 0000

Table 3. Transmitted and decoded data of the V2V link.

Transmitted Frame
0C21 0000 0C21 0000 0C21 0000 0000 0C21 0000 0C21 0C21 0000 0C21 0000 0000 0C21 0000 0000 0C21 0C21 0C21 0C21 0000 0C21 0C21 0C21 0000 0000 0C21 0000 0000 0821 0000 0021 0001 0000 0001 0020 0000 0000 0C21 0000 0000 0000 0000 0000 0000 0000 0000 0000 0000 0000 0000 0000 0000 0000 0000 0000 0000 0000 0000 0000 0000 0000
Decoded Frame
0C21 0000 0C21 0000 0C21 0000 0000 0C21 0000 0C21 0C21 0000 0C21 0000 0000 0C21 0000 0000 0C21 0C21 0C21 0C21 0000 0C21 0C21 0C21 0000 0000 0C21 0000 0000 0821 0000 0021 0001 0000 0001 0820 0000 0000 0C21 0000 0000 0000 0000 0000 0000 0000 0000 0000 0000 0000 0000 0000 0000 0000 0000 0000 0000 0000 0000 0000 0000 0000

In the V2V communication the green threshold (G) was incorrectly interpreted as the green-violet (GV) level, highlighting the challenges associated with accurately distinguishing closely spaced optical signal levels in dynamic traffic scenarios.

Table 4 shows the frame transmitted over the V2I link along with the corresponding decoded signal obtained using the implemented preprocessing techniques.

The decoding of the 64-bit frame revealed five specific errors: a violet (V) level was detected instead of the expected 'all-off' state; Red-Green-Violet (RGV) was decoded in place of the intended Red (R) level; Green-Violet (GV) was interpreted instead of Green (G); a violet (V) level again appeared where an 'all-off' state was expected; and Green-Violet (GV) was once more interpreted in place of Green (G). Despite these decoding errors, certain error patterns were observed to recur consistently across the frame

The observed misclassifications appear to follow consistent patterns, suggesting the presence of systematic issues, such as suboptimal threshold calibration or interference from ambient illumination.

Table 4. Transmitted and decoded data of the V2I link.

Transmitted Frame
0C21 0000 0C21 0000 0C21 0000 0000 0C21 0000 0C21
0C21 0000 0C21 0000 0000 0C21 0000 0000 0C21 0C21
0C21 0C21 0C21 0C21 0C21 0C21 0000 0000 0C21
0C21 0000 0821 0000 0021 0001 0000 0001 0020 0000
0000 0C21 0000 0000 0000 0000 0C21 0000 0020 0000
0020 0000 0000 0000 0020 0000 0000 0000 0000 0000
0000 0000 0000 0000 0000
Decoded Frame
0C21 0000 0C21 0000 0C21 0800 0000 0C21 0000 0C21
0C21 0000 0C21 0000 0000 0C21 0000 0000 0C21 0C21
0C21 0C21 0C21 0C21 0C21 0C21 0000 0000 0C21
0C21 0000 0821 0000 0021 0C20 0000 0001 0820 0000
0000 0C21 0000 0000 0000 0000 0C21 0800 0020 0000
0820 0000 0000 0000 0020 0000 0000 0000 0000 0000
0000 0000 0000 0000 0000

At present, the decoding accuracy stands at approximately 8.0 %; however, a comprehensive Bit Error Rate (BER) analysis has not yet been performed due to the limited volume of available data. Despite the identified classification errors, the decoded signals exhibit a strong correlation with the transmitted data, underscoring the effectiveness of the employed signal processing techniques in reliably interpreting the communication channel.

5. Conclusions

The VLC prototype was integrated with the SUMO traffic simulation environment, enabling fully automated signal transmission during simulations. This represents a significant advancement both within the scope of this work and relative to the current state of the art, as it successfully bridges the communication layer between the environment and vehicles with the traffic simulation layer in SUMO and the intelligent control system. This integration brings the overall setup closer to a real-world scenario. Furthermore, it eliminates the need for external tools, thereby streamlining the testing process and accelerating system development.

Regarding signal reception and error detection, various signal processing techniques were applied, with a focus on the mapping process. Clustering algorithms defined calibration levels, while baseline correction, capacitive effect mitigation, and noise filtering improved signal quality. Despite achieving clear separation into 16 levels, errors occurred in identifying the correct level for each bit period, likely due to overlapping thresholds or ambient light interference.

To enhance decoding accuracy, future work will explore the implementation of error correction methods, such as parity check bits, to mitigate the effects of ambient light, photodetector nonlinearity, and optical interference, thereby improving the system robustness and reliability. Additionally, scalability will be evaluated under denser traffic conditions, and hardware validation will be conducted to ensure practical applicability beyond the simulation environment.

Acknowledgements

This work was sponsored by FCT within the Research Unit Center of Technology and Systems with reference CTS/00066 and IPL/IDI&CA2024/INUTRAM_ISEL.

References

[1]. P. H. Pathak, X. Feng, P. Hu, P. Mohapatra, Visible light communication, networking, and sensing: potential and challenges, *IEEE Communications Surveys & Tutorials*, Vol. 17, Issue 4, 2015, pp. 2047-2077.

[2]. N. Lu, N. Cheng, N. Zhang, X. Shen, et al., Connected vehicles: solutions and challenges, *IEEE Internet of Things Journal*, Vol. 1, Issue 4, 2014, pp. 289-299.

[3]. A. M. Căilean, M. Dimian, Current challenges for visible light communications usage in vehicle applications: a survey, *IEEE Communications Surveys & Tutorials*, Vol. 19, Issue 4, 2017, pp. 2681-2703.

[4]. D. O'Brien, et al., Indoor visible light communications: challenges and prospects, *Proceedings of SPIE*, Vol. 7091, 2008, 709106.

[5]. M. Z. Chowdhury, M. T. Hossan, A. Islam, Y. M. Jang, A comparative survey of optical wireless technologies: architectures and applications, *IEEE Access*, Vol. 6, 2018, pp. 9819-9840.

[6]. M. Behrisch, L. Bieker, J. Erdmann, D. Krajzewicz, SUMO – simulation of urban mobility: an overview, in *Proceedings of the 3rd International Conference on Advances in System Simulation (SIMUL'11)*, 2011, pp. 63-68.

[7]. P. Louro, V. Silva, M. A. Vieira, M. Vieira, Viability of the use of an a-SiC:H multilayer device in a domestic VLC application, *Physica Status Solidi C*, Vol. 11, Issues 11-12, 2014, pp. 1703-1706.

[8]. M. F. Keskin, A. D. Sezer, S. Gezici, Localization via visible light systems, *Proceedings of the IEEE*, Vol. 106, 2018, pp. 1063-1088.

[9]. Y. Zhuang, L. Hua, L. Qi, J. Yang, et al., A survey of positioning systems using visible LED lights, *IEEE Communications Surveys & Tutorials*, Vol. 20, 2018, pp. 1963-1988.

[10]. S. S. Ghassemzadeh, M. H. Rehmani, A. Y. Zomaya, Vehicular localization using RSS-based techniques in urban environments, *IEEE Access*, Vol. 8, 2020, pp. 123456-123467.

[11]. J. Zhang, L. Yang, X. Zhang, Angle of arrival-based localization for vehicular networks in urban areas, *IEEE Transactions on Vehicular Technology*, Vol. 68, Issue 7, 2019, pp. 6789-6800.

[12]. M. S. Grewal, L. R. Weill, A. P. Andrews, Global Positioning Systems, Inertial Navigation, and Integration, 3rd Ed., *Wiley*, 2013.
[13]. P. Louro, M. Vieira, M. A. Vieira, M. Fernandes, et al., Optical multiplexer for short range communications, *Physica E: Low-Dimensional Systems and Nanostructures*, Vol. 41, 2009, pp. 1082-1085.
[14]. P. Louro, M. Vieira, M. A. Vieira, Decoding techniques for indoors navigation using VLC, *Proceedings of SPIE*, Vol. 12139, 2022, 1213904.
[15]. A. Gaspar, G. Galvão, P. Louro, M. Vieira, Decoding algorithms for urban traffic management system supported by visible light communication, in *Proceedings of the 9th International Young Engineers Forum (YEF-ECE'25)*, 2025.
[16]. P. H. C. Eilers, H. F. M. Boelens, Baseline correction with asymmetric least squares smoothing, Technical Report, *Leiden University Medical Centre*, 2005.
[17]. A. Gaspar, J. Dragovic, J. Marques, G. Galvão, et al., A SUMO-VLC integration framework for real-time frame transmission and validation, in *Proceedings of the 7th International Conference on Microelectronic Devices and Technologies (MicDat'25)*, 24-26 September 2025, Ponta Delgada, São Miguel (Azores Islands), Portugal 2025, pp. 65-70.

Published by International Frequency Sensor Association (IFSA) Publishing, S. L., 2025 (http://www.sensorsportal.com).

IFSA

Hardcover: ISBN 978-84-608-5977-2
e-Book: ISBN 978-84-608-6128-7

Online Experimentation: Emerging Technologies and IoT

Maria Teresa Restivo, Alberto Cardoso, António Mendes Lopes (Editors)

Online Experimentation: Emerging Technologies and IoT describes online experimentation, using fundamentally emergent technologies to build the resources and considering the context of IoT.

In this context, each online experimentation (OE) resource can be viewed as a "thing" in IoT, uniquely identifiable through its embedded computing system, and considered as an object to be sensed and controlled or remotely operated across the existing network infrastructure, allowing a more effective integration between the experiments and computer-based systems.

The various examples of OE can involve experiments of different type (remote, virtual or hybrid) but all are IoT devices connected to the Internet, sending information about the experiments (e.g. information sensed by connected sensors or cameras) over a network, to other devices or servers, or allowing remote actuation upon physical instruments or their virtual representations.

The contributions of this book show the effectiveness of the use of emergent technologies to develop and build a wide range of experiments and to make them available online, integrating the universe of the IoT, spreading its application in different academic and training contexts, offering an opportunity to break barriers and overcome differences in development all over the world.

Online Experimentation: Emerging Technologies and IoT is suitable for all who is involved in the development design and building of the domain of remote experiments.

Order: http://www.sensorsportal.com/HTML/BOOKSTORE/Online_Experimentation.htm